Simulating Convection

Hanon Theo
LMECA2660
theo.hanon@student.uclouvain.be

March 12, 2024

1 Discretize Periodic Domain

We explore the effect of domain size L on the approximation of Discrete Fourier Transform (DFT) coefficients to the Fourier coefficients in an unbounded domain. We present a comparison of DFT coefficients and their approximation in **Fig.**1. Since the signal is real and periodic, resulting in a symmetric spectrum, we only display one half of it. We

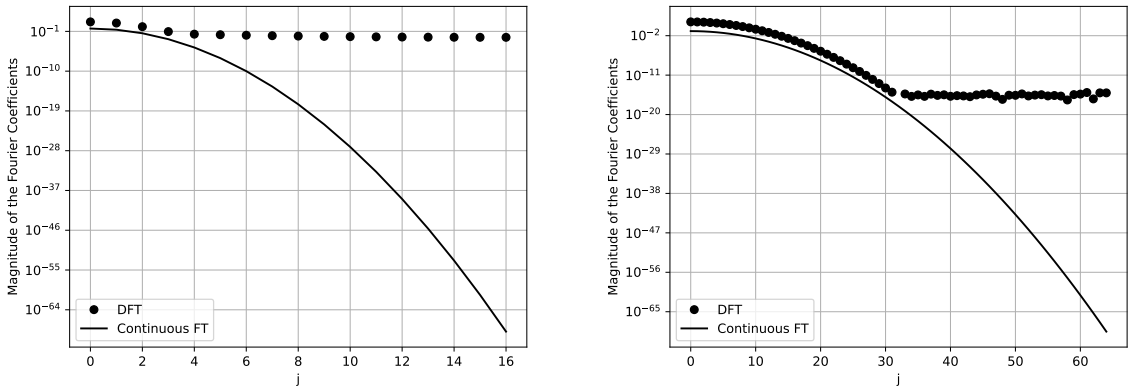

(a) $\frac{L}{\sigma} = 4$ (b) $\frac{L}{\sigma} = 16$

Figure 1: Comparison between the Discrete and Continuous Fourier Coefficients of a Gaussian function with $\frac{h}{\sigma} = 1/8$ and $\mu = 0$. We considered $N = 128$ grid points for the DFT.

find that a lower ratio of $\frac{L}{\sigma}$, where σ represents the Gaussian's standard deviation, leads to a more accurate approximation of the DFT coefficients. This accuracy is influenced by the fact that DFT coefficients are calculated within a window of size L, ignoring any information beyond this window. When the ratio is $\frac{L}{\sigma} = 4$, significant data is lost, resulting in an approximation that quickly deviates from the exact DFT coefficients. In contrast, with a ratio of $\frac{L}{\sigma} = 16$, the Gaussian width is much smaller compared to the domain size. This smaller width allows the approximation to accurately represent about half of the wavenumbers. Although the approximation for the remaining wavenumbers is less precise, the magnitudes of these coefficients are generally small, making the overall approximation still satisfactory.

2 Partially Decentred Scheme

In order to obtain a finite difference scheme involving $u_i, u_{i+1}, u_{i-1}, u_{i-2}$ we shall start with the taylor expensions of $u_{i+1}, u_{i-1}, u_{i-2}$:

$$\begin{aligned}
u_{i+1} &= u_i + h\frac{\partial u_i}{\partial x} + \frac{h^2}{2}\frac{\partial^2 u_i}{\partial x^2} + \frac{h^3}{6}\frac{\partial^3 u_i}{\partial x^3} + \frac{h^4}{24}\frac{\partial^4 u_i}{\partial x^4} + O(h^5),\\
u_{i-1} &= u_i - h\frac{\partial u_i}{\partial x} + \frac{h^2}{2}\frac{\partial^2 u_i}{\partial x^2} - \frac{h^3}{6}\frac{\partial^3 u_i}{\partial x^3} + \frac{h^4}{24}\frac{\partial^4 u_i}{\partial x^4} - O(h^5),\\
u_{i-2} &= u_i - 2h\frac{\partial u_i}{\partial x} + 2\frac{h^2}{2}\frac{\partial^2 u_i}{\partial x^2} - \frac{8h^3}{6}\frac{\partial^3 u_i}{\partial x^3} + \frac{16h^4}{24}\frac{\partial^4 u_i}{\partial x^4} + O(h^5).
\end{aligned}$$

We want to find the best linear combination (i.e. $\alpha u_{i+1} + \beta u_{i-1} + \gamma u_{i-2}$) such that we cancel out the most high order terms possible. In this case, the best we can do is to cancel out the 2nd and 3th order terms. Indeed if we want to get rid of the 4th order term it would have been necessary to solve a homogeneous 3x3 non singular linear system which would have led to trivial coefficients. Therefore, the system to solve is

$$\begin{cases}
\frac{\alpha}{2} + \frac{\beta}{2} + \gamma &= 0\\
\\
\frac{\alpha}{6} - \frac{\beta}{6} - \frac{8\gamma}{6} &= 0,
\end{cases}$$

which yields $\alpha = \frac{1}{2},\ \beta = -3,\ \gamma = 1$. Combining everything we have

$$c\left(\frac{1}{2}u_{i-2} - 3u_{i-1} + u_{i+1}\right) = c\left(-\frac{3}{2}u_i + 3h\frac{\partial u_i}{\partial x} + \frac{h^4}{4}\frac{\partial^4 u_i}{\partial x^4} + O(h^5)\right),$$

that can be further simplify as

$$c\frac{\partial u_i}{\partial x} = c\left(\frac{3u_i + u_{i-2} - 6u_{i-1} + 2u_{i+1}}{6h}\right) - \frac{ch^3}{12}\frac{\partial^4 u_i}{\partial x^4} + O(h^5).$$

In summary, we have a scheme of order 3 with a truncation error term given by $\frac{ch^3}{12}\frac{\partial^4 u_i}{\partial x^4}$.

Now, given that $u_i(t) = \sum_j \hat{U}_j(t)e^{ik_j x_i}$ and $\frac{d\hat{U}_j}{dt} = \lambda_j \hat{U}_j$, we can compute an expression of λ_j for our scheme. We start with the convection equation, in which we use our scheme to approximate the spatial derivative :

$$\begin{aligned}
\frac{\partial u}{\partial t} &= -c\frac{\partial u_i}{\partial x}\\
&= -c\left(\frac{3u_i + u_{i-2} - 6u_{i-1} + 2u_{i+1}}{6h}\right).
\end{aligned}$$

Thereafter, we can inject the expression of $u_i(t)$ and it gives

$$\sum_j \lambda_j \hat{U}_j e^{ik_j x_i} = \sum_j -\frac{c}{h}\hat{U}_j e^{ik_j x_i}\left[\frac{1}{2} + \frac{1}{6}e^{-2ik_j h} - e^{-ik_j h} + \frac{1}{3}e^{ik_j h}\right].$$

Finally we identify according to the indices to obtain

$$\lambda_j = -\frac{c}{h}\left[\frac{1}{2} + \frac{1}{6}e^{-2ik_j h} - e^{-ik_j h} + \frac{1}{3}e^{ik_j h}\right]$$

We introduce the modified wavenumber k^*, it reprents the error commited by the approximation. More precisely, we assume that

$$\begin{aligned}\hat{U}ik^*e^{ikx_i} &= -c\frac{\partial u_i}{\partial x} \\ &= -\frac{c}{h}\hat{U}e^{ikx_i}\left[\frac{1}{2}+\frac{1}{6}e^{-2ikh}-e^{-ikh}+\frac{1}{3}e^{ikh}\right],\end{aligned}$$

where we considered only one mode for simplicity. Note that if k^* were exactly equal to k, our scheme would be exact[1]. However, since it isn't the case in practise, we will next compare the modified wave number with the real one. One can obtain by further simplifying the previous expression :

$$k^*h = \left(\frac{1}{6}\sin(2kh)-\frac{4}{3}\sin(kh)\right)+i\left(\frac{1}{2}+\frac{1}{6}\cos(2kh)-\frac{2}{3}\cos(kh)\right).$$

Interestingly, k^*h is not purely imaginary, as it also possesses a complex part. This means that the scheme introduces not only dispersion error but also amplitude errors into the solution. It is important to remember that we are examining the convection equation, where diffusion in our solution is not expected. The comparison between the magnitudes and phases of the approximated and exact wave numbers is illustrated in **Fig.**2. Regarding the magnitude, it is noted that the approximation remains relatively

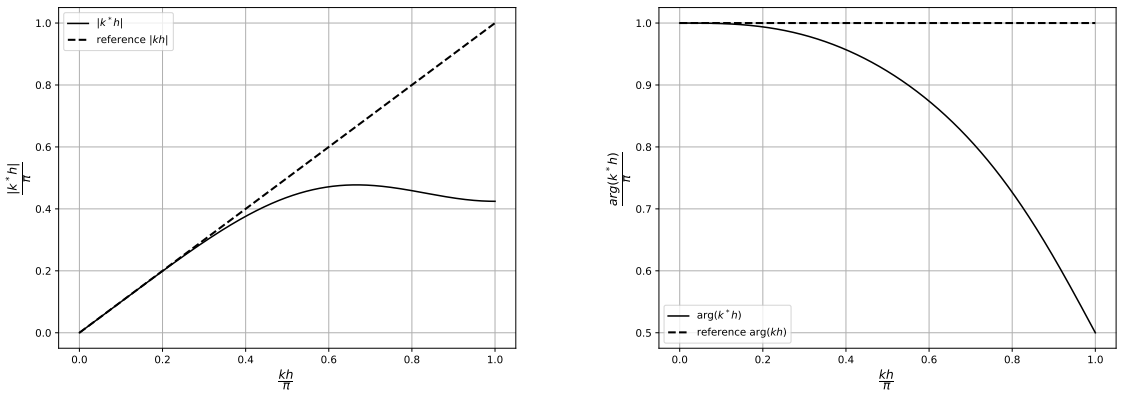

(a) (b)

Figure 2: (a) Magnitude (b) Phase of $\frac{k^*h}{\pi}$ as a function of $\frac{kh}{\pi}$.

accurate up to $\frac{kh}{\pi} = 0.3$, closely aligning with the expected value of $\frac{kh}{\pi}$. Beyond this point, however, the approximation deteriorates significantly, indicating that modes with high wavenumber will propagate at speeds different from c. A similar trend is observed in the phase behavior: initial modes exhibit correct behavior, but the accuracy begins to decline at an even earlier stage than with the magnitude. This leads to diffusion in the solution, a phenomenon that is inconsistent with the characteristics of a convection equation.

[1]Indeed, $\frac{\partial u_i}{\partial x} = \hat{U}ike^{ikx_i}$.

3 Stability

Before starting the computation of the maximum CFL of each scheme, let us make a quick recap of how we are going the proceed. We first seek for λ_{max} of each scheme by upper bounding each individual term of the expression of λ_j. Given that we are working with RK4 we need that $\lambda_{max}\Delta t \leq 2\sqrt{2}$. We also know that

$$\begin{aligned}\lambda_{max}\Delta t &= \frac{\lambda_{max}h}{c}\frac{c\Delta t}{h} \\ &= \left(\frac{\lambda_{max}h}{c}\right) CFL.\end{aligned}$$

We can then impose the condition for the stability of RK4 and get

$$CFL \leq \frac{c}{\lambda_{max}h}2\sqrt{2}$$

Note that λ_{max} is an upper bound (possibly strict) on the maximum λ_j in magnitude. In the following computation, we shall consider that c is positive and we shall write λ and k instead of λ_j and k_j to simplify notations.

3.1 E2

We start form the expression of λ for E2 :

$$\begin{aligned}\lambda &= -\frac{ic}{h}\sin(kh) \\ \implies |\lambda| &= \frac{c}{h}|\sin(kh)| \\ \implies \lambda_{max} &= \frac{c}{h}\end{aligned}$$

Finally, we get that $CFL_{E2} \leq 2\sqrt{2}$.

3.2 E4

The expression of λ is

$$\lambda = -i\frac{c}{h}\left[\frac{4}{3}\sin kh - \frac{1}{6}\sin 2kh\right]$$

We can bound $\sin(kh)$ and $-\sin(2kh)$ by 1 even thought those values will never be reached at the same time, this is why λ_{max} may be a strict bound. We get

$$\lambda_{max} = \frac{c}{h}\left[\frac{4}{3} + \frac{1}{6}\right] = \frac{3}{2}\frac{c}{h}.$$

Therefore, $CFL_{E4} \leq \frac{4\sqrt{2}}{3}$.

3.3 I4

The expression of λ is

$$\lambda = -i\frac{c}{h}\left[\frac{\frac{3}{2}\sin(kh)}{1+\frac{1}{2}\cos(kh)}\right]$$

The latter can be bound by

$$\begin{aligned}\lambda_{max} &= \frac{c}{h}\left[\frac{\frac{3}{2}}{1-\frac{1}{2}}\right] \\ &= \frac{3c}{h}\end{aligned}$$

We get then $CFL_{I4} \leq \frac{2\sqrt{2}}{3}$

3.4 ED

Finally, we can start from the expression we found earlier

$$\lambda = -\frac{c}{h}\left[\frac{1}{2} + \frac{1}{6}e^{-2ikh} - e^{-ikh} + \frac{1}{3}e^{ikh}\right]$$

We can bound individually the magnitude of each each exponential by 1 (or -1 depending of the sign) which give

$$\begin{aligned}\lambda_{max} &= \frac{c}{h}\left[\frac{1}{2} + \frac{1}{6} + 1 + \frac{1}{3}\right] \\ &= \frac{2c}{h}\end{aligned}$$

which lead to $CFL_{ED} \leq \sqrt{2}$

In conclusion, to ensure a margin of safety, we opt to conservatively round down $\sqrt{2}$ to $\frac{7}{5}$ when determining the upper limit. We then select the smallest CFL number from our list (with the round down applied to it), which is $CFL = \frac{14}{15} \approx 0.993$. This choice is further validated by examining **Fig.**3, where it is clear that the $\lambda\Delta t$ values for each scheme remain well within the stability region delineated by the Runge-Kutta 4 (RK4) method ; we even have a big safety margin.

4 Numerical Simulation & Analysis of the Result

4.1 Analysis of the Results

We examine the simulation results at the finest resolution first i.e. $\frac{h}{\sigma} = 0.125$, shown in the **Fig.**4. Overall, each simulation compares well with the exact solution. Specifically, the approximation obtained using I4 and E4 schemes are really close to the analytical solution and show no dispersion errors. However, the simulation using the ED scheme shows some diffusion over time, which is expected due to the scheme's decentered nature that introduces amplitude error. Nevertheless, the ED scheme does not exhibit dispersion

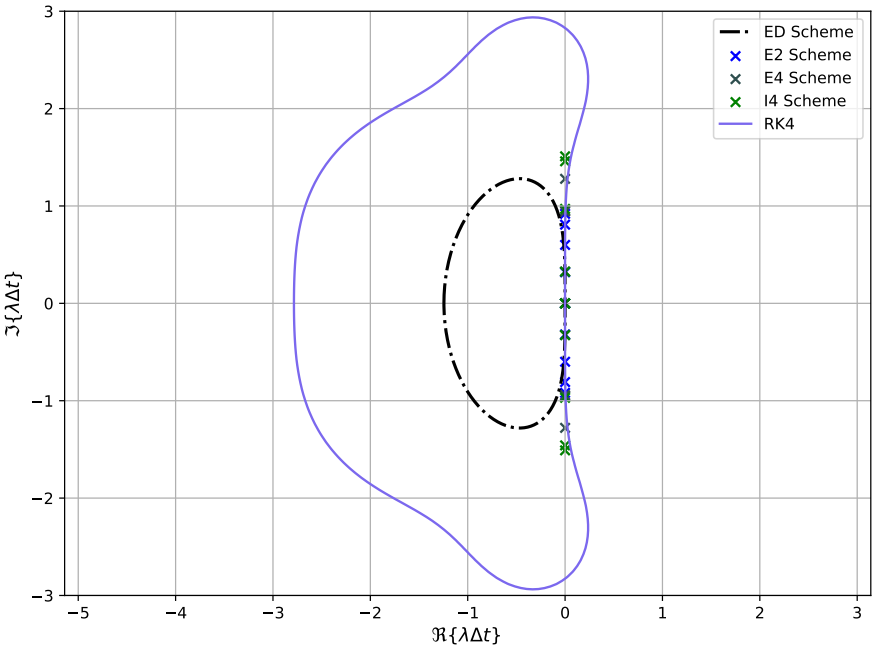

Figure 3: Stability region of the RK4 integration scheme (red curve) and $\lambda\Delta t$ values taken by the schemes E2, E4, ED, I4 for $CFL = \frac{14}{15}$. For clarity we only considered 10 values of $\lambda\Delta t$ for E2, E4, I4.

errors. Unsurprisingly, the E2 scheme delivers the worst results. At time $\frac{ct}{L} = 1/2$, we can see a small offset between the approximation and the solution ; it indicates dispersion errors. By the time $\frac{ct}{L} = 1$, it gets worse, some spatial modes are left behind. Even though the E2 and ED schemes have errors, they are still satisfactory approximations because of the fine resolution of the grid. Now, we'll move on to simulations with coarser resolutions, where the approximations are expected to be less accurate.

We consider the case $\frac{h}{\sigma} = 0.250$, as illustrated in the **Fig.**5, we observe different levels of accuracy among the simulation schemes. The I4 scheme continues to provide a highly accurate solution, showing its robustness even on the coarser grid. The E4 scheme, however, begins to display slight dispersion errors by $\frac{ct}{L} = 1$, though it remains a reasonable approximation at $\frac{ct}{L} = \frac{1}{2}$. The issues previously noted for the ED and E2 schemes have become more pronounced. Specifically, the ED scheme now shows diffusion at both $\frac{ct}{L} = \frac{1}{2}$ and 1, with minor dispersion errors also noticeable at $\frac{ct}{L} = 1$. The E2 scheme suffers from major dispersion errors as early as $\frac{ct}{L} = \frac{1}{2}$, indicating a substantial decrease in approximation accuracy at this resolution; at the point that the numerical solution provided by the E2 scheme cannot be considered reliable.

We focus to the coarser grid of $\frac{h}{\sigma} = 0.5$, the result are on **Fig.**6, the overall quality of the simulations deteriorates significantly. Among them, the E4 scheme performs the best, yet it starts showing small dispersion errors as early as $\frac{ct}{L} = \frac{1}{2}$. The same conclusions apply to the simulation with E4 scheme but the dispersions are even more marked. The ED scheme is starting to undergo dispersion but the errors is mainly due to the amplitude issues. As for the E2 scheme, the approximation quality is extremely poor; by $\frac{ct}{L} = \frac{1}{2}$, the original shape of the function is lost due to severe dispersion, resulting in the

initial condition being broken down into multiple modes.

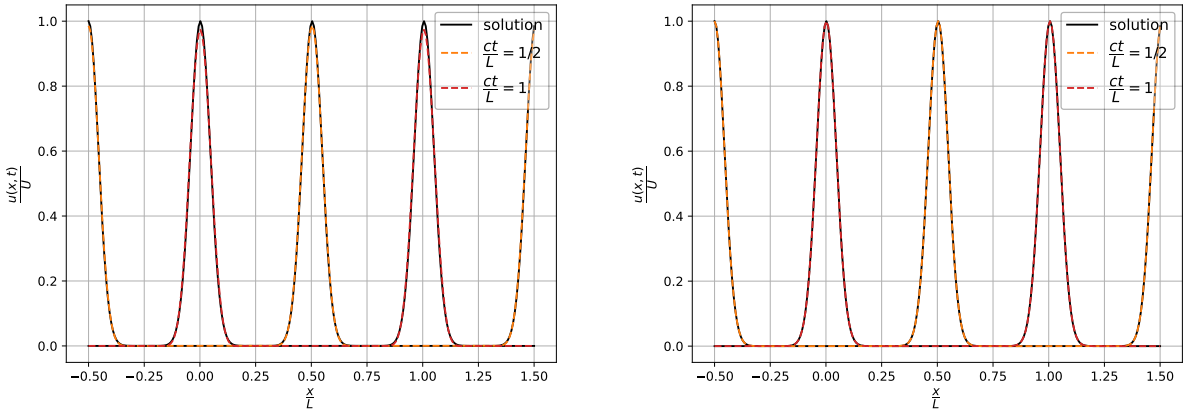

(a) ED scheme

(b) I4 scheme

(c) E2 scheme

(d) E4 scheme

Figure 4: Comparison at $\frac{h}{\sigma} = 0.125$ between the exact solution and the numerical simulation with $CFL = 0.5$ across schemes (ED, I4, E2, E4).

4.2 Global Diagnoses

The global diagnostics for each method are depicted in **Fig.**7. We first examine the I_h^n diagnostic. It's noted that I_h^n is consistent across all schemes and for any value of $\frac{h}{\sigma}$, indicating that every method adequately conserves the integral of the initial condition This result aligns with our understanding of dispersion and amplitude errors. Specifically, dispersion errors cause the various modes of the initial condition to spread out, and amplitude errors lead to the spreading of the initial condition itself. Therefore, neither type of error impacts the integral.

Recall that E_h^n is an empirical measure of the energy contained within the function. Therefore, a decreasing E_h^n indicates that the convection process is not perfectly efficient and dissipates energy. The E2, E4, and I4 schemes show low energy dissipation over time; energy is conserved at $\frac{h}{\sigma} = \frac{1}{8}$, and there are minor losses for $\frac{h}{\sigma} = \frac{1}{2}$ and $\frac{1}{4}$, with E2 being the most conservative among them. This suggests that for these schemes, dissipation is attributable to the temporal scheme, explaining why E2 is the most conservative;

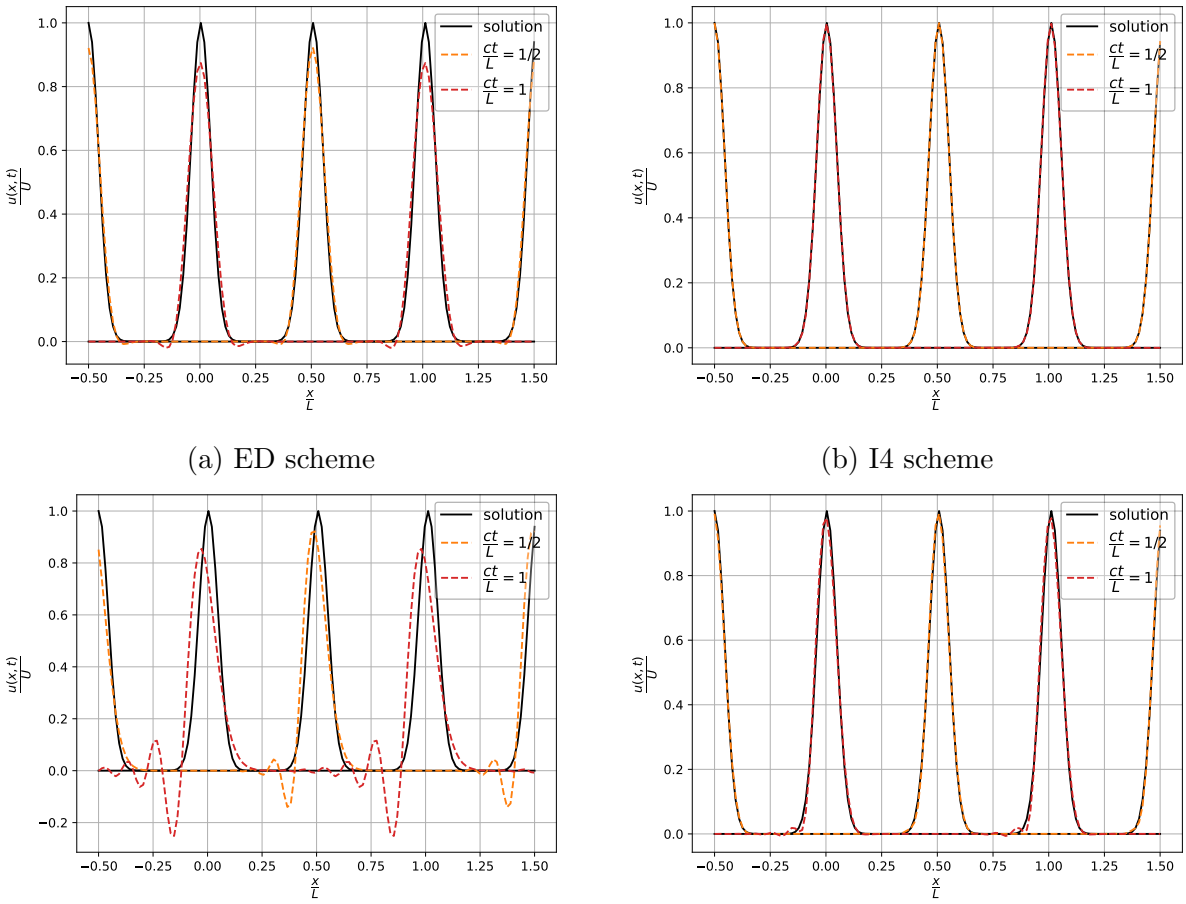

(a) ED scheme

(b) I4 scheme

(c) E2 scheme

(d) E4 scheme

Figure 5: Comparison at $\frac{h}{\sigma} = 0.250$ between the exact solution and the numerical simulation with $CFL = 0.5$ across schemes (ED, I4, E2, E4).

higher-order schemes are more prone to instabilities. In contrast, the ED scheme experiences significant dissipation effects at all considered $\frac{h}{\sigma}$ values, failing to conserve energy. This is due to diffusion caused by the scheme's; diffusion process does not conserve energy.

Based on the empirical global error R_h^n, the methods rank in accuracy as follows: I4, ED, E4, and E2, with E4 significantly outperforming the others. Its error is an order of magnitude lower than the rest and it displayed a significantly better convergence speed. The ED and E4 schemes exhibit similar error magnitudes, with ED performing better at $\frac{h}{\sigma} = \frac{1}{2}$ and E4 excelling at $\frac{h}{\sigma} = \frac{1}{4}$. This difference highlights the superior convergence rate of E4. Both methods converge to the solution at $\frac{h}{\sigma} = \frac{1}{8}$. The E2 scheme, however, fails to reach the solution, demonstrating a lower convergence rate compared to the others. This outcome is expected, given that E2 is the method of lowest order.

4.3 Order of Convergence

The empirical curve depicting the global error is presented in **Fig.**8, calculated across a range of $\frac{h}{\sigma}$ values to thoroughly evaluate complexity. The figure also includes the

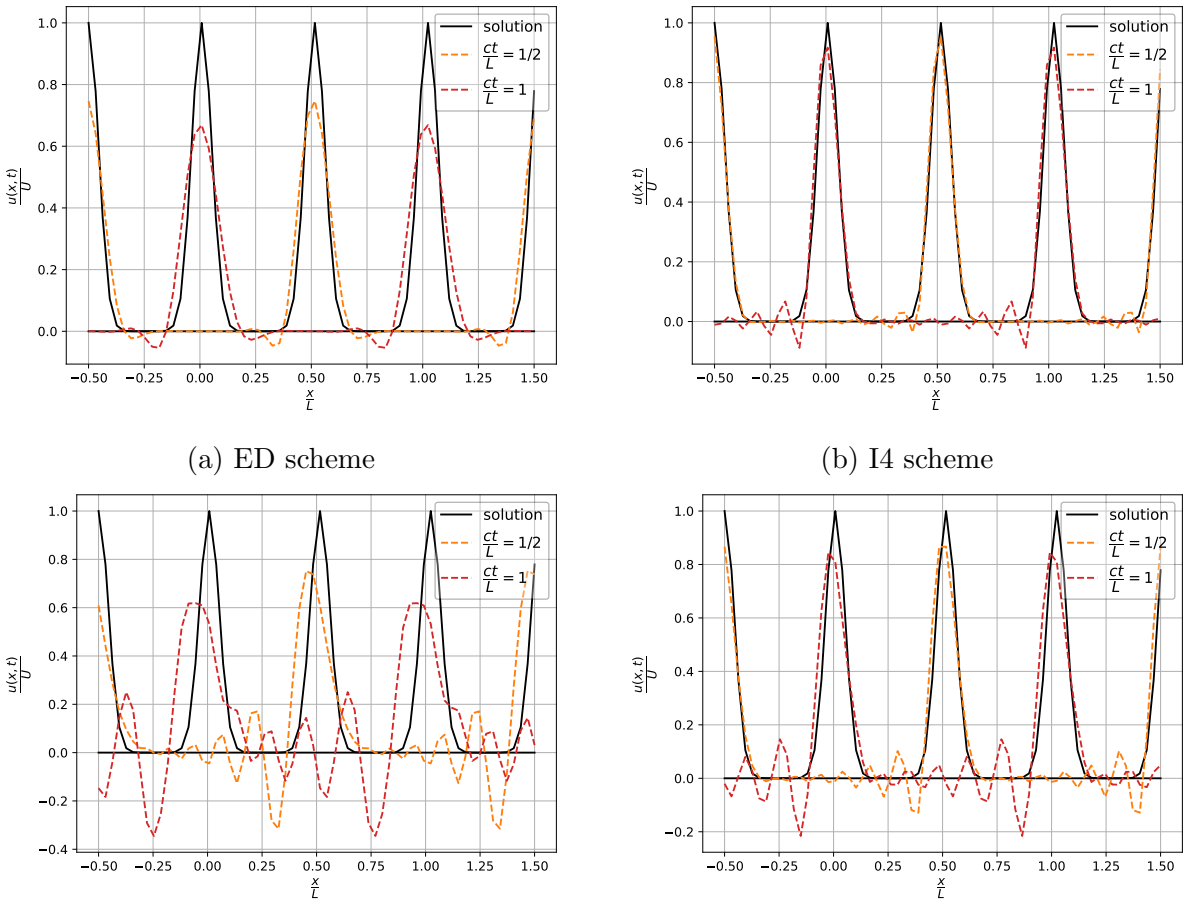

(a) ED scheme

(b) I4 scheme

(c) E2 scheme

(d) E4 scheme

Figure 6: Comparison at $\frac{h}{\sigma} = 0.500$ between the exact solution and the numerical simulation with $CFL = 0.5$ across schemes (ED, I4, E2, E4).

empirically determined complexity bound that best matches the observed data. Given that R_h^n is proportional to the sum of square of the error at each measurement point, the true complexity order should be divided by 2. This is due to the fact that squaring the error in a logarithmic scale increases the slope by a factor of 2. Therefore, the empirical complexity bounds are consistent with the theoretical predictions. These findings are summarized in Tab.1.

Scheme	**Complexity Order** $\mathcal{O}(\cdot)$
E2	h^2
E4	h^4
I4	h^4
ED	h^3

Table 1: Complexity Order of Each Scheme

4.4 Non Uniform Grid

We want to re-write the transport equation w.r.t. a new function $v(\xi, t)$ and a non uniform speed $b(\xi)$ such that we can use do simulations on a uniform grid. Let us start

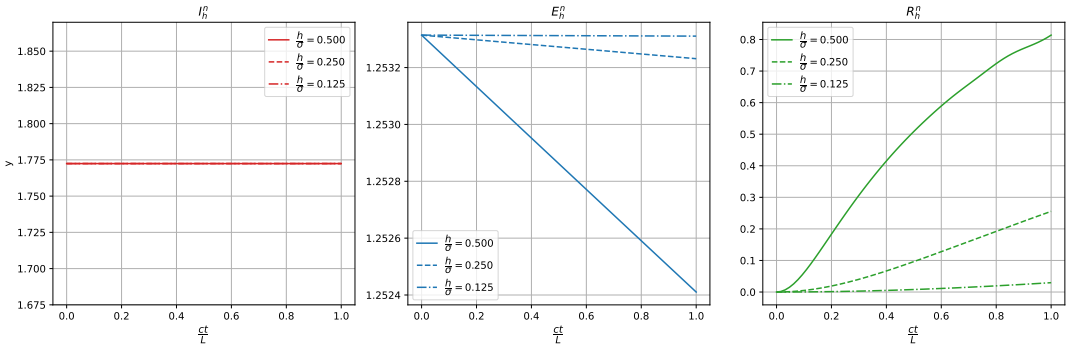

(a) E2 scheme

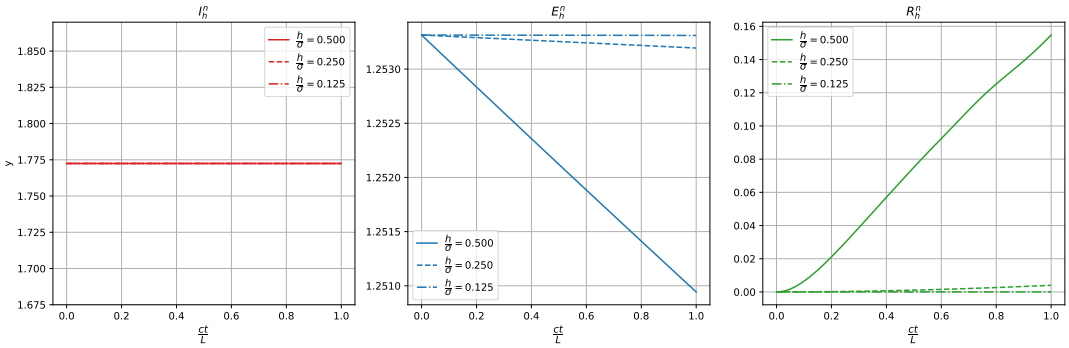

(b) E4 scheme

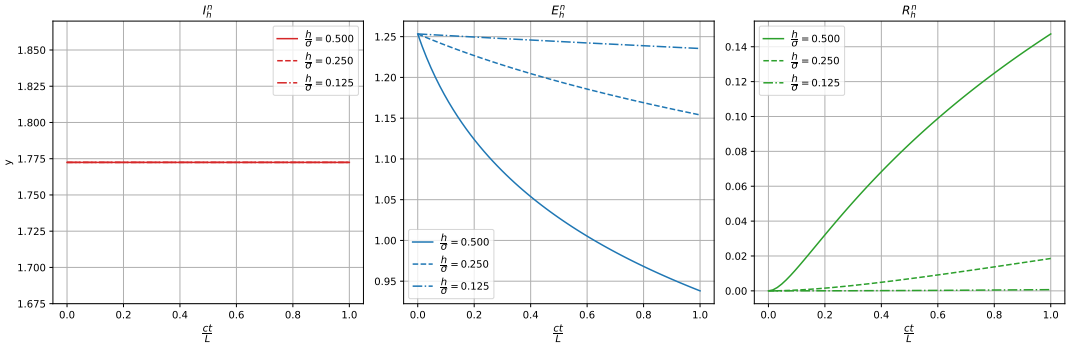

(c) ED scheme

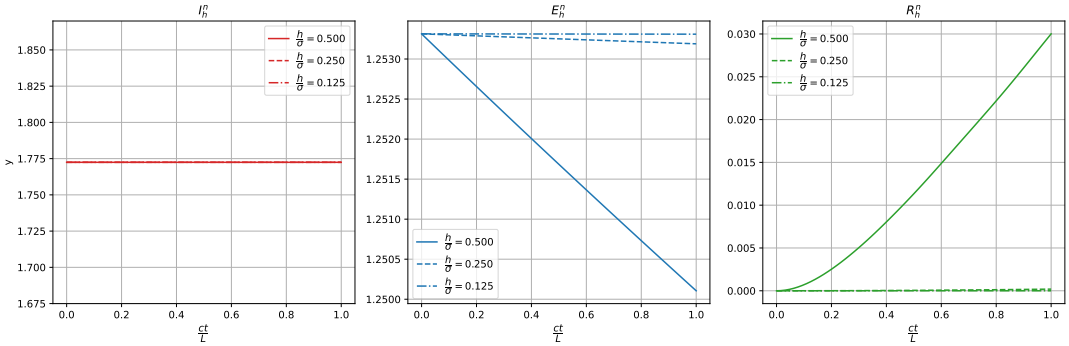

(d) I4 scheme

Figure 7: Global diagnoses $I_h^n,\ E_h^n,\ R_h^n$ across schemes (E2, E4, ED, I4) with $CFL = 0.5$ for $\frac{ct}{L} \in [0, 1]$.

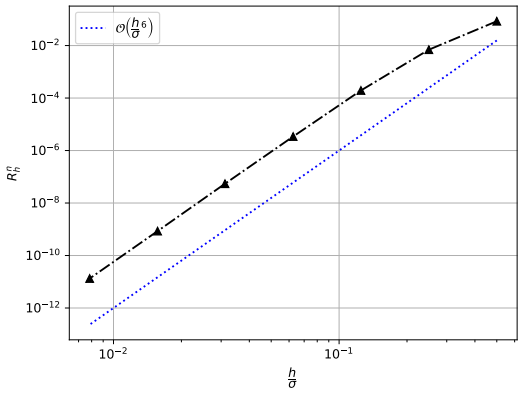

(a) ED scheme

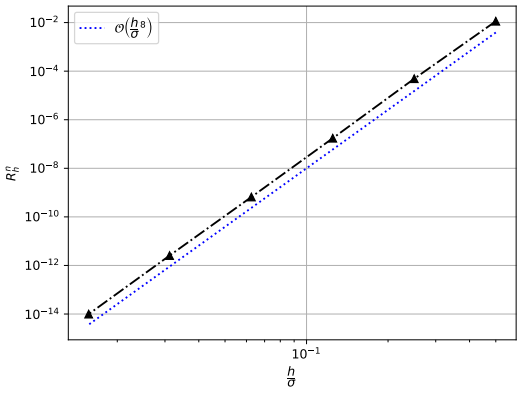

(b) I4 scheme

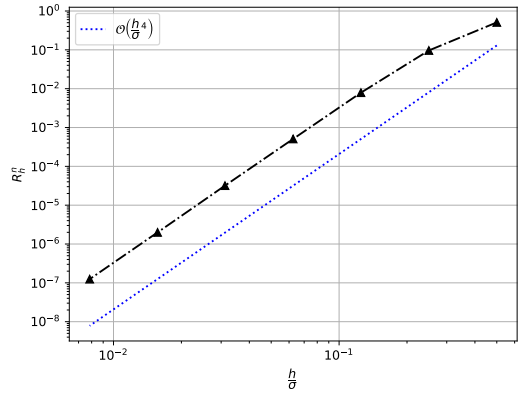

(c) E2 scheme

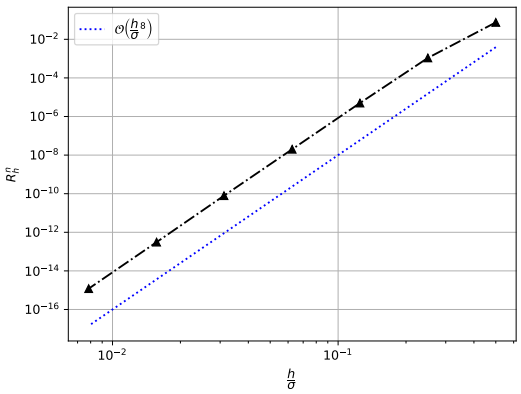

(d) E4 scheme

Figure 8: LogLog plot of the empirical error R_h^n at $\frac{ct}{L} = \frac{1}{2}$ and the respective theoretical complexity of each scheme; we computed R_h^n on $\frac{h}{\sigma} = \frac{1}{2},\ \frac{1}{4},\ \frac{1}{8},\ \frac{1}{16},\ \frac{1}{32}$.

with the equation and apply the chain rule to the spatial derivative

$$\frac{\partial u}{\partial t} + c\frac{\partial u}{\partial \xi}\frac{d\xi}{dx} = 0.$$

Recall the mapping between the physical and numerical space

$$x = g(\xi) = \xi - a\frac{L}{2\pi}\sin\left(2\pi\frac{\xi}{L}\right),$$

we can develop the mapping's derivate and get

$$\frac{\partial u}{\partial t} + \frac{c}{1 - a\cos\left(2\pi\frac{\xi}{L}\right)}\frac{\partial u}{\partial \xi} = 0.$$

We can then multiply on both side by $g'(\xi)$ to obtain

$$\frac{\partial}{\partial t}\left(\left[1 - a\cos\left(2\pi\frac{\xi}{L}\right)\right]u(g(\xi),t)\right) + \frac{\partial}{\partial \xi}\left(\frac{c}{1 - a\cos\left(2\pi\frac{\xi}{L}\right)}\left[1 - a\cos\left(2\pi\frac{\xi}{L}\right)\right]u(g(\xi),t)\right) = 0$$

Finally by identification, one can obtain

$$\begin{cases} b(\xi) = & c\left[g'(\xi)\right]^{-1} \\ v(\xi,t) = & g'(\xi)\ u(g(\xi),t) \end{cases}$$

where

$$g'(\xi) = 1 - a\cos\left(2\pi\frac{\xi}{L}\right).$$

The simulation can thus be performed on the uniform grid by being careful to initialize $v(\xi, t)$ accordingly with the expression obtained. We can then recover $u(x, t)$ by inverting the equation above.

The equation obtained

$$\frac{\partial v}{\partial t} + \frac{\partial}{\partial \xi}\Big(b(\xi)v(\xi, t)\Big) = 0,$$

is conservative; it means that the integral of v is conserved over time. In mathematical words it is that

$$\frac{d}{dt}\int_{-L/2}^{L/2} v(\xi, t)d\xi = 0.$$

We shall proof this property. We start from the above integrale and since the support of the integral don't vary over time we can inverse it with the time derivative and get

$$\begin{aligned}\frac{d}{dt}\int_{-L/2}^{L/2} v(\xi, t)d\xi &= \int_{-L/2}^{L/2}\frac{\partial v}{\partial t}d\xi. \\ &= \int_{-L/2}^{L/2} -\frac{\partial}{\partial \xi}\Big(b(\xi)v(\xi, t)\Big)d\xi \\ &= -\Big[b(\xi)v(\xi, t)\Big]_{-L/2}^{L/2} = 0.\end{aligned}$$

The last expression assumes that $v(\xi, t)$ is zero at the boundaries; in the case of the Gaussian/wavepacket this is an approximation which get better with $\frac{L}{\sigma}$ growing. Since the speed $b(\xi)$ is non uniform we will see an interesting behavior of the numerical solution to conserve its integral.

4.4.1 Gaussian Initial Condition

The numerical solutions for each scheme are depicted in **Fig.**10, while the corresponding physical solutions are presented in **Fig.**9. In terms of the physical solution's quality, we observe a consistent trend with simulations conducted on a uniform grid. The I4 and E4 schemes closely match the actual solution, whereas the ED and E2 schemes exhibit significant amplitude and dispersion errors, respectively, more so than in the uniform grid case. Regarding the numerical solution, the comment done about the precision of the simulations are applicable. What is interesting though is that the function undergoes considerable shape changes over time, attributed to the conservation property discussed earlier. As the function moves through areas of lower speed, it peaks to maintain its integral. Conversely, in faster regions, it spreads to preserve its integral.

The error amplification mentioned stems from the equation's conservative form, requiring the function to adjust depending on speed variations, leading to significant shape changes. These abrupt alterations in shape are challenging to accurately capture, even with a fine grid, resulting in increased errors. An alternate approach to understanding the error is to remark that the Fourier coefficients needs to constantly adapt their amplitudes. This alteration can magnify modes that were previously insignificant in the original Gaussian, these amplified modes then deteriorates the error (since we know that modes with high k_j are prone to bigger errors).

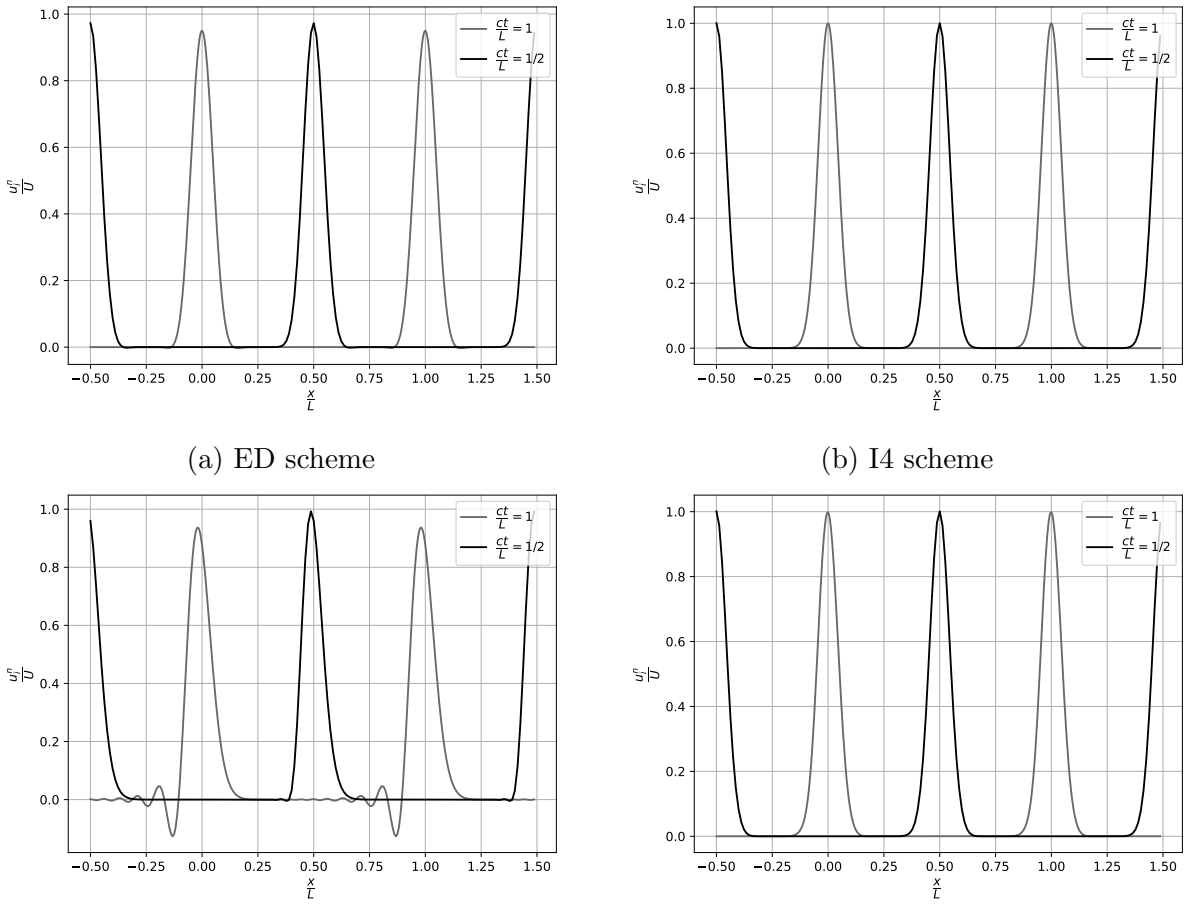

(a) ED scheme

(b) I4 scheme

(c) E2 scheme

(d) E4 scheme

Figure 9: Plot of $\frac{u_i^n}{U}$ with $CFL = 0.5$, $\frac{h}{\sigma} = 0.125$ for $\frac{ct}{L} = \frac{1}{2}$, 1 across schemes (ED, I4, E2, E4). Simulation has been conducted on a non-uniform grid with parameter $a = \frac{3}{5}$.

4.4.2 Wave Packet Initial Condition

We study the same simulation trick but with an initial condition given by a Wave Packet (WP). Before doing so, we would like to analyse possible oncoming errors in the simulation, we will thus examine the WP's spectrum and its group velocity.

The WP's spectrum is shown on **Fig.**11. The spectrum is essentially double the Gaussian spectrum, with each part centered at the cosine's positive and negative frequencies. This happens because of the Fourier Transform properties: multiplying in the space domain turns into convolving in the Fourier domain, and the Fourier Transform of a cosine results

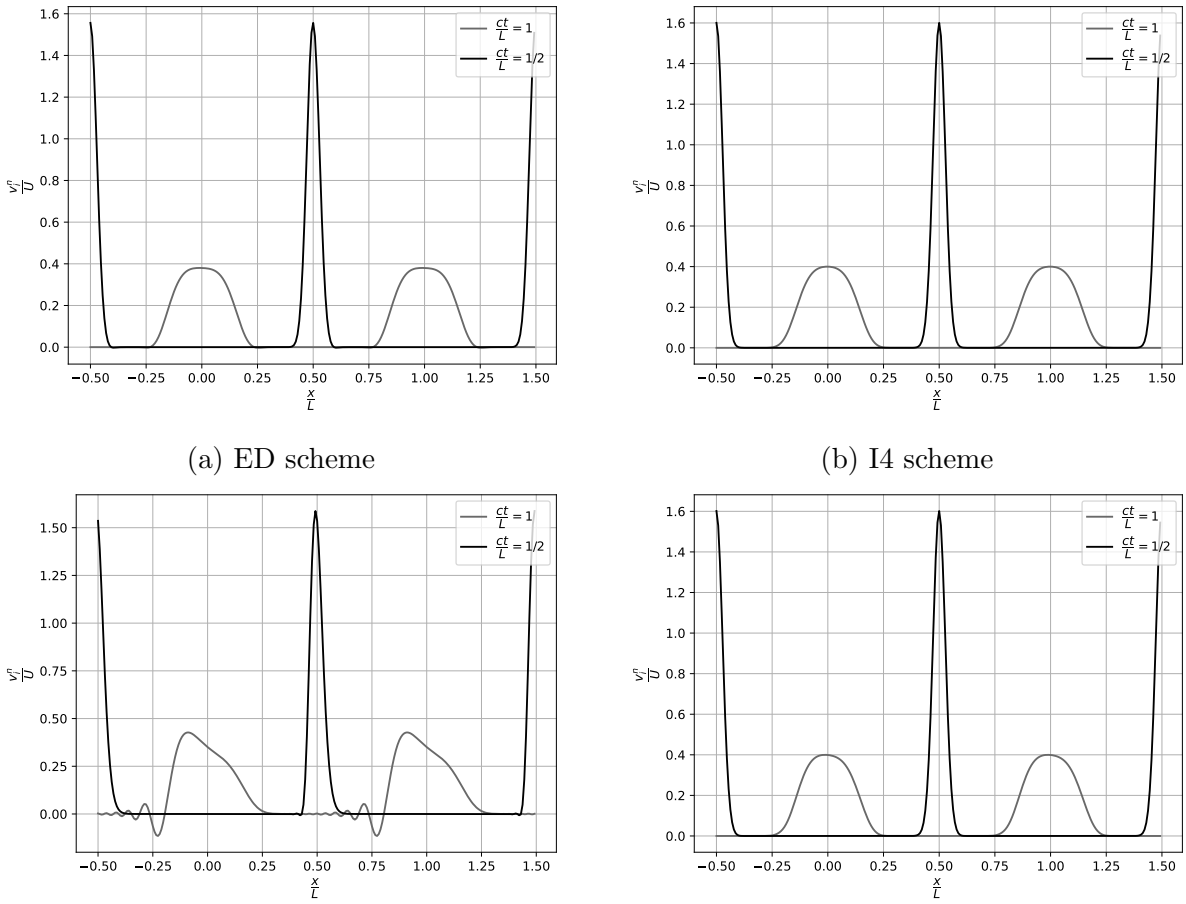

(a) ED scheme

(b) I4 scheme

(c) E2 scheme

(d) E4 scheme

Figure 10: Plot of $\frac{v_i^n}{U}$ with $CFL = 0.5$, $\frac{h}{\sigma} = 0.125$ for $\frac{ct}{L} = \frac{1}{2},\ 1$ across schemes (ED, I4, E2, E4). Simulation has been conducted on a non-uniform grid with parameter $a = \frac{3}{5}$.

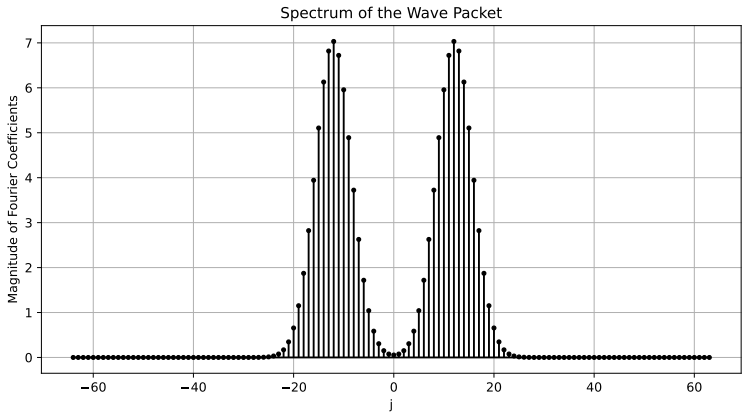

Figure 11: Spectrum of a wave packet with $p = 12$ and $N = 128$.

in two spikes (Dirac deltas) at the cosine's frequencies. Since convolving with a Dirac's delta just shifts the position, the Gaussian spectrum is moved to these two frequencies. The main problem now is that the spatial modes, where the simulation is accurate (i.e. the small wavenumbers), have small Fourier coefficients and are therefore insignificant. This

means the wavenumbers where the simulation makes big errors are the most significant ones. Because of this, we expect higher dispersion and amplitude errors in the simulation.

In **Fig.**12, we show the group velocity for different schemes. We notice that all the

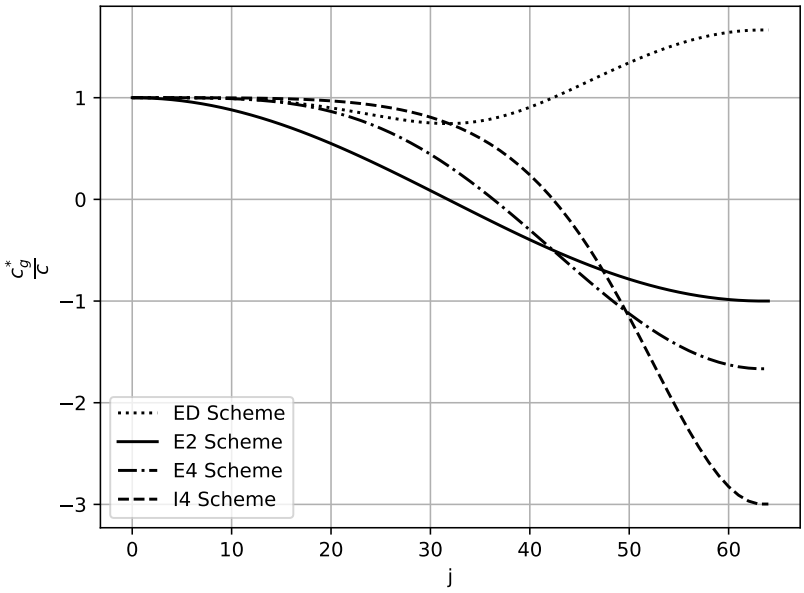

Figure 12: Group velocity for each scheme with $N = 128$

centered schemes eventually develop a negative group velocity as j increases. A negative group velocity is not physically realistic, so we prefer this behavior to occur at only a few frequencies (j as large as possible). Among the schemes, E2 is the first to exhibit a negative c_g^*, followed by E4, and then I4. Although I4 is the last to become negative, its decrease is very sharp, and it reaches a significantly negative value towards the end. Regarding the ED scheme, the ratio $\frac{c_g^n}{c}$ initially shows a slight decrease but then returns exactly to one at $j = 42$. After this point, it continues to increase, making the group velocity faster than the actual group velocity for those wavenumbers. Among the scheme, ED is the one that matches the best the real group velocity for almost all values of j. However, it's important to note that this scheme introduces amplitude errors, which could be analyzed by examining the "phase" velocity of the Wave Packet (WP), though this aspect won't be discussed here. When we look at the spectrum (refer to **Fig.**11), the most significant wavenumbers range from $-25 \leq j \leq 25$. By comparing this with the group velocities shown in **Fig.**12, we can conclude that the simulation results for each scheme will be moved in the correct direction. For this particular setup ($p = 12$), the E2 scheme is anticipated to have the weakest performance in terms of matching the group velocity. It will be followed by E4, then the ED scheme, with the I4 scheme expected to deliver the most accurate results.

The results of the experiment are displayed in **Fig.**13. As predicted, the E2 scheme performs the worst, experiencing significant dispersion errors along with an incorrect group velocity from as early as $\frac{ct}{L} = \frac{1}{4}$. By the time $\frac{ct}{L} = \frac{1}{2}$, the Wave Packet (WP) has noticeably shifted from the exact solution. The E4 scheme, while maintaining a group

velocity closer to the expected value than E2, still suffers from minor dispersion errors at $\frac{ct}{L} = \frac{1}{4}$, and these errors become more pronounced by $\frac{ct}{L} = \frac{1}{2}$. The ED scheme accurately matches the exact group velocity as anticipated, but it displays significant amplitude errors; at $\frac{ct}{L} = \frac{1}{2}$, the amplitude is reduced by at least half. Finally, the E4 scheme not only follows the correct group velocity closely but also exhibits only minor dispersion by $\frac{ct}{L} = \frac{1}{2}$. This scheme is clearly the best choice for this specific task.

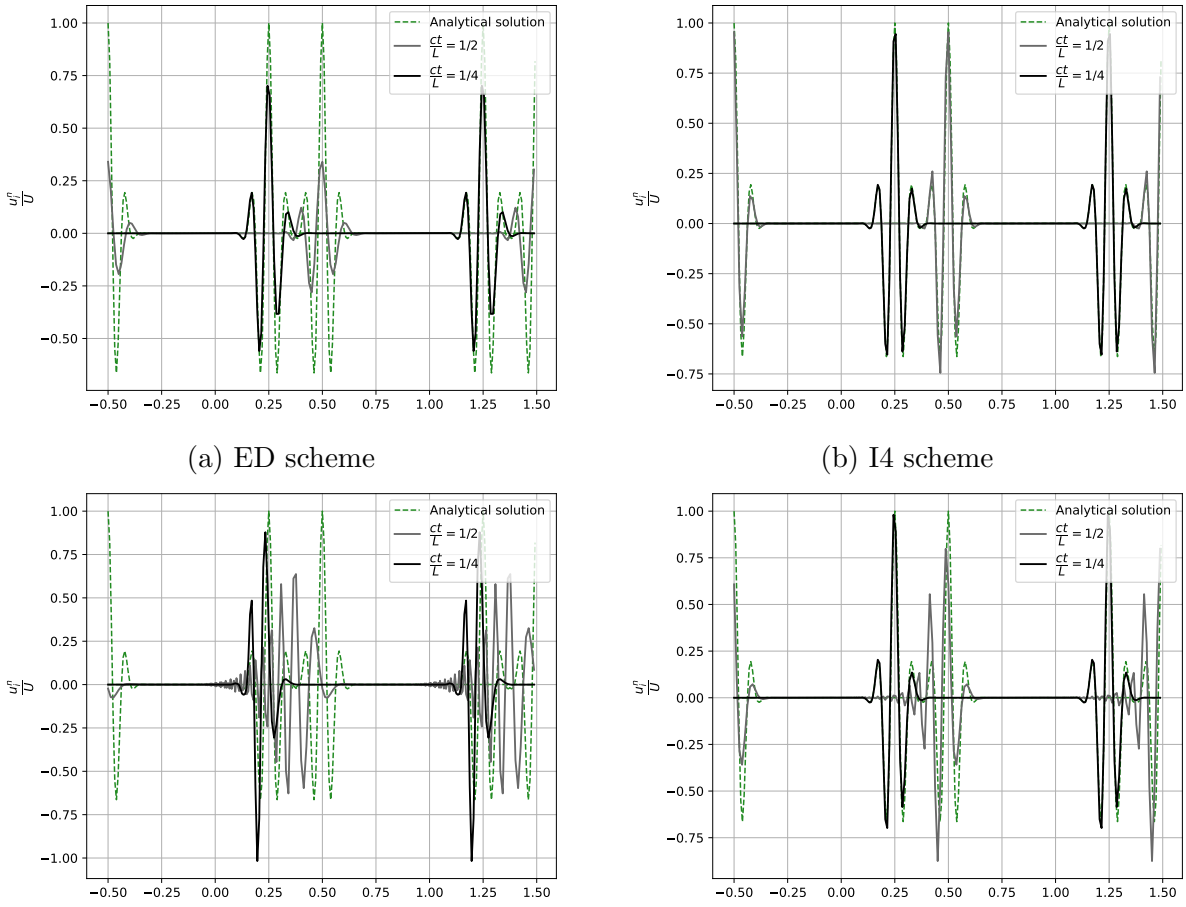

(a) ED scheme

(b) I4 scheme

(c) E2 scheme

(d) E4 scheme

Figure 13: Plot of $\frac{u_i^n}{U}$ and $\frac{u(x_i,t^n)}{U}$ with $CFL = 0.5$, $\frac{h}{\sigma} = 0.125$ for $\frac{ct}{L} = \frac{1}{4}, \frac{1}{2}$ across schemes (ED, I4, E2, E4). Initial condition is given by a wave packet with $p = 12$. Simulation has been conducted on a non-uniform grid with parameter $a = \frac{3}{5}$.